An Assessment of High-Order-Mode Analysis and Shape Optimization of Expansion Chamber Mufflers

Min-Chie CHIU[1], Ying-Chun CHANG[2]

[1] *Department of Mechanical and Automation Engineering, Chung Chou University of Science and Technology*
6, Lane 2, Sec. 3, Shanchiao Rd., Yuanlin, Changhua 51003, Taiwan, R.O.C.; e-mail: minchie.chiu@msa.hinet.net

[2] *Department of Mechanical Engineering, Tatung University*
No. 40, Sec. 3, Zhongshan N.Rd., Taipei 104, Taiwan, R.O.C.; e-mail: ycchang@ttu.edu.tw

A substantial quantity of research on muffler design has been restricted to a low frequency range using the plane wave theory. Based on this theory, which is a one-dimensional wave, no higher order wave has been considered. This has resulted in underestimating acoustical performances at higher frequencies when doing muffler analysis via the plane wave model. To overcome the above drawbacks, researchers have assessed a three-dimensional wave propagating for a simple expansion chamber muffler. Therefore, the acoustic effect of a higher order wave (a high frequency wave) is considered here. Unfortunately, there has been scant research on expansion chamber mufflers equipped with baffle plates that enhance noise elimination using a higher-order-mode analysis. Also, space-constrained conditions of industrial muffler designs have never been properly addressed. So, in order to improve the acoustical performance of an expansion chamber muffler within a constrained space, the optimization of an expansion chamber muffler hybridized with multiple baffle plates will be assessed.

In this paper, the acoustical model of the expansion chamber muffler will be established by assuming that it is a rigid rectangular tube driven by a piston along the tube wall. Using an eigenfunction (higher-order-mode analysis), a four-pole system matrix for evaluating acoustic performance (STL) is derived. To improve the acoustic performance of the expansion chamber muffler, three kinds of expansion chamber mufflers (KA-KC) with different acoustic mechanisms are introduced and optimized for a targeted tone using a genetic algorithm (GA). Before the optimization process is performed, the higher-order-mode mathematical models of three expansion chamber mufflers (A-C) with various allocations of inlets/outlets and various chambers are also confirmed for accuracy. Results reveal that the STL of the expansion chamber mufflers at the targeted tone has been largely improved and the acoustic performance of a reverse expansion chamber muffler is more efficient than that of a straight expansion chamber muffler. Moreover, the STL of the expansion chamber mufflers will increase as the number of the chambers that separate with baffles increases.

Keywords: higher order wave, eigenfunction, optimization, genetic algorithm.

1. Introduction

RAYLEIGH (1945) and HARTING & SWANSON (1938) initiated analyzing the effect of a higher order sound. Thereafter, MILES (1944) stretched the acoustic performance of higher order waves at the discontinuity section of the muffler. In 1945, based on the plane wave theory, DAVIS (1954) assessed mufflers and experimentally investigated the plane wave phenomenon. He found that a wave propagated along a duct can be regarded as a plane wave when the duct size is smaller than the wave length of the sound wave. Later, IGARASHI, TOYAMA, MIWA, and ARAI (1958, 1959, 1960) successfully analyzed a muffler's acoustical performance using a four-pole transfer matrix. Additionally, MUNJAL (1957) deduced the advanced four-pole transfer matrix using the fluid dynamic theory. SULLIVAN and CROCKER (1978, 1979) developed coupled equations for the outer and inner tubes of a perforated muffler. In 1981, JAYARAMAN and YAM (1981) provided an analytic solution for the coupled equations; however, all the solutions were obtained on the basis of the plane wave theory, where the accuracy of the analytic solution became worse

for a higher order wave (a higher frequency wave). To overcome this drawback, IH and LEE (1985, 1987) proposed the acoustic performance of an expansion muffler with a circular section. The design of bias at the inlet and outlet of the muffler created two kinds of mufflers (a straight and reverse ones).

MUNJAL (1987) simplified the calculation process using a numerical analysis method. ABOM (1990) also suggested using absorbing end plates in the expansion chamber. In addition, it is hard to analyze a muffler using the analytic method if the angle between inlet and outlet is 90 degrees. This type of muffler is also often assessed using the finite element method (YOUNG, CROCKER, 1975) or the two-dimensional boundary element method (SEYBERT, CHENG, 1987). Nevertheless, the calculation time is long. IH (1992) used the numerical method to analyze the acoustic performance of the expansion muffler hybridized with a circular section/rectangular section inlet/outlet duct. The inlet/outlet duct may be parallel with/without the same height and perpendicular to each other. To quickly search for the appropriate design parameters, CHANG et al. (2004a; 2004b) assessed the acoustic performance of space-constrained single expansion mufflers (with/without sound absorbing material inside the wall) using the GA method. ELSAADANY et al. (2011) assessed the optimization of exhaust systems for a band of noise.

As mentioned above, the expansion chamber muffler used in the numerical and analytic approach is simply shaped. The noise reduction of mufflers is not high. In addition, the temperature of the venting gas passing through the traditional plenum chamber that equips with absorbing baffles is often very high. It will cause the absorbing material erode easily; therefore, application of sound absorbing material lined inside a plenum chamber is limited and will not be used in the study. In order to enhance the acoustic performance and endurance of the expansion chamber mufflers, three kinds of mufflers (KA: a concentric straight muffler; KB: a reverse straight muffler; KC: a straight muffler hybridized with two non-absorbing baffles) with no absorbing material lining are proposed and applied in noise reduction using the GA method.

2. Theoretical background

For a rectangular expansion chamber muffler with no noise source located inside a chamber, the acoustical model is established by assuming that it is a rigid rectangular tube and is driven by a piston along the tube wall. A quiet medium with non-viscous and thermal-isolated properties fills the chamber. Concerning the higher order wave, the mathematical models of two expansion chamber mufflers with different allocations of inlets and outlets shown in Figs. 1 and 2 will be deduced in Subsec. 2.1. In order to enhance the acoustic
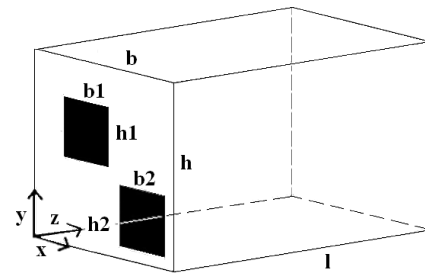

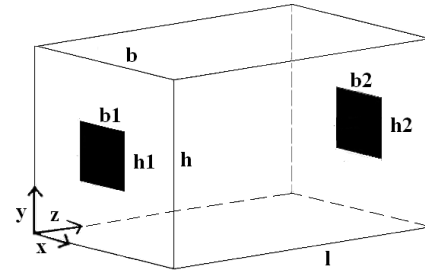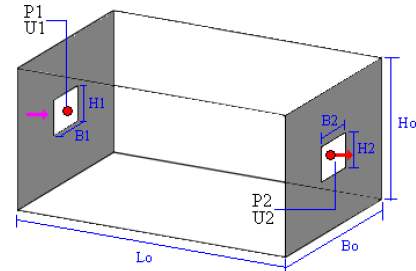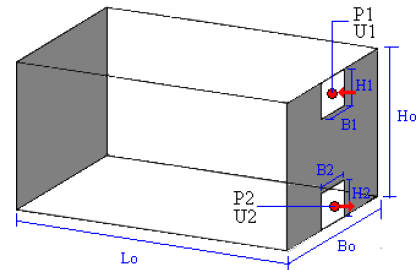Fig. 1. Mechanism of a reverse expansion chamber muffler.

Fig. 2. Mechanism of a straight expansion chamber muffler.
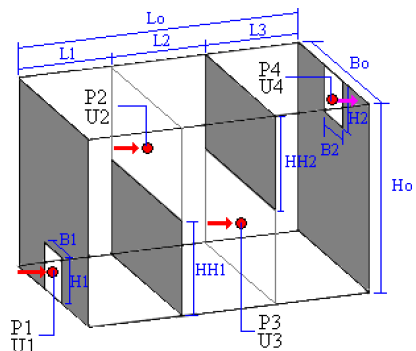
a) muffler KA

b) muffler KB

c) muffler KC

Fig. 3. Mechanisms for three kinds of expansion chamber mufflers (muffler KA: a concentric straight expansion chamber muffler; muffler KB: a reverse straight expansion chamber muffler; muffler KC: a straight expansion chamber muffler hybridized with two baffles).

performance of the expansion chamber muffler, three kinds of mufflers (KA: a concentric straight expansion chamber muffler; KB: a reverse straight expansion chamber muffler; KC: a straight expansion chamber muffler hybridized with two baffles) with different mechanisms shown in Fig. 3 are proposed. Based on the analysis of the higher order modes, the acoustic performances of mufflers (KA, KB, and KC) will be established in Subsec. 2.2. Finally, the objective functions of the three mufflers at a target tone will be described in Subsec. 2.3.

2.1. Derivation of mathematical models

The three-dimensional governing equation of the sound wave for a rectangular expansion chamber muffler shown in Figs. 1 and 2 is derived by IH (1992). The inlet and outlet are on the same side or on different sides shown in Figs. 1. The inlet's acoustic pressure ($\overline{p}_{11}$) is expressed as

$$\overline{p}_{11} = (-1)^1 jU_1 Z_0 \left\{ \frac{1}{\tan kl} + \left(\frac{bh}{b_1 h_1} \right)^2 \right.$$

$$\cdot \left[\sum \frac{1}{v_{m0}} \left(\frac{2}{m\pi} \right)^2 \left(\frac{h_1}{h} \right)^2 \psi_{111}^2 \right.$$

$$+ \sum \frac{1}{v_{0n}} \left(\frac{2}{n\pi} \right)^2 \left(\frac{b_1}{b} \right)^2 \psi_{112}^2$$

$$\left. + \sum\sum \frac{1}{v_{mn}} \left(\frac{4}{mn\pi^2} \right)^2 \psi_{111}^2 \psi_{112}^2 \right] \quad (1)$$

$$\left. \cdot \frac{k}{k_z \tan k_z l} \right\} = (-1)^1 jU_1 Z_0 E_{11},$$

$$\psi_{111} = \sin \frac{m\pi b_1}{2b} \cos \frac{m\pi b_{c1}}{b},$$

$$\psi_{112} = \sin \frac{m\pi h_1}{2h} \cos \frac{m\pi h_{c1}}{h},$$

where b is the width of the expansion chamber, h is its height, l is its length, b_1 is the width of the inlet, h_1 is the height of the inlet, (b_{c1}, h_{c1}) is the centre coordinate of the inlet, $k \left(= \frac{\omega}{c_o} \right)$ is the wave number of the sound wave, $k_z \left(= \sqrt{k^2 - k_x^2 - k_y^2} \right)$ is the wave number of the sound wave in z-axis, $k_x \left(= \frac{m\pi}{b} \right)$ is the wave number of the sound wave in x-axis, $k_y \left(= \frac{n\pi}{h} \right)$ is the wave number of the sound wave in y-axis, m, n are the acoustic modes, U_1 is the volume velocity at node 1, Z_0 is the acoustic impedance of the expansion chamber in z-axis.

Similarly, the outlet's acoustic pressure ($\overline{p}_{22}$) is expressed as (IH, 1992)

$$\overline{p}_{22} = (-1)^2 jU_2 Z_0 \left\{ \frac{1}{\tan kl} + \left(\frac{bh}{b_2 h_2} \right)^2 \right.$$

$$\cdot \left[\sum \frac{1}{v_{m0}} \left(\frac{2}{m\pi} \right)^2 \left(\frac{h_2}{h} \right)^2 \psi_{221}^2 \right.$$

$$+ \sum \frac{1}{v_{0n}} \left(\frac{2}{n\pi} \right)^2 \left(\frac{b_2}{b} \right)^2 \psi_{222}^2$$

$$\left. + \sum\sum \frac{1}{v_{mn}} \left(\frac{4}{mn\pi^2} \right)^2 \psi_{221}^2 \psi_{222}^2 \right] \quad (2)$$

$$\left. \cdot \frac{k}{k_z \tan k_z l} \right\} = (-1)^2 jU_2 Z_0 E_{22},$$

$$\psi_{221} = \sin \frac{m\pi b_2}{2b} \cos \frac{m\pi b_{c2}}{b},$$

$$\psi_{222} = \sin \frac{m\pi h_2}{2h} \cos \frac{m\pi h_{c2}}{h},$$

where b_2 is the width of the outlet, h_2 is the height of the outlet, (b_{c2}, h_{c2}) is the centre coordinate of the outlet, U_2 is the volume velocity at node 2.

When the inlet and outlet are on the same side, the interactive average acoustic pressures ($\overline{p}_{12}$ and $\overline{p}_{21}$) are (IH, 1992)

$$\overline{p}_{12} = (-1)^2 jU_2 Z_0 \left\{ \frac{1}{\tan kl} + \left(\frac{bh}{b_1 h_1} \right) \left(\frac{bh}{b_2 h_2} \right) \right.$$

$$\cdot \left[\sum \frac{1}{v_{m0}} \left(\frac{2}{m\pi} \right)^2 \left(\frac{h_1}{h} \right) \left(\frac{h_2}{h} \right) \psi_{121} \psi'_{121} \right.$$

$$+ \sum \frac{1}{v_{0n}} \left(\frac{2}{n\pi} \right)^2 \left(\frac{b_1}{b} \right) \left(\frac{b_2}{b} \right) \psi_{122} \psi'_{122}$$

$$\left. + \sum\sum \frac{1}{v_{mn}} \left(\frac{4}{mn\pi^2} \right)^2 \psi_{121} \psi'_{121} \psi_{122} \psi'_{122} \right]$$

$$\left. \cdot \frac{k}{k_z \tan k_z l} \right\} = (-1)^2 jU_2 Z_0 E_{12},$$

$$(3)$$

$$\overline{p}_{21} = (-1)^1 jU_1 Z_0 \left\{ \frac{1}{\tan kl} + \left(\frac{bh}{b_2 h_2} \right) \left(\frac{bh}{b_1 h_1} \right) \right.$$

$$\cdot \left[\sum \frac{1}{v_{m0}} \left(\frac{2}{m\pi} \right)^2 \left(\frac{h_2}{h} \right) \left(\frac{h_1}{h} \right) \psi_{211} \psi'_{211} \right.$$

$$+ \sum \frac{1}{v_{0n}} \left(\frac{2}{n\pi} \right)^2 \left(\frac{b_2}{b} \right) \left(\frac{b_1}{b} \right) \psi_{212} \psi'_{212}$$

$$\left. + \sum\sum \frac{1}{v_{mn}} \left(\frac{4}{mn\pi^2} \right)^2 \psi_{211} \psi'_{211} \psi_{212} \psi'_{212} \right]$$

$$\left. \cdot \frac{k}{k_z \tan k_z l} \right\} = (-1)^1 jU_1 Z_0 E_{21}.$$

As indicated in Fig. 2, when the inlet and outlet are on the opposite side, the interactive average acoustic pressures ($\overline{p}_{12}$ and $\overline{p}_{21}$) are (IH, 1992)

$$\overline{p}_{12} = (-1)^2 jU_2 Z_0 \left\{ \frac{1}{\sin kl} + \left(\frac{bh}{b_1 h_1} \right) \left(\frac{bh}{b_2 h_2} \right) \right.$$

$$\cdot \left[\sum \frac{1}{v_{m0}} \left(\frac{2}{m\pi} \right)^2 \left(\frac{h_1}{h} \right) \left(\frac{h_2}{h} \right) \psi_{121} \psi'_{121} \right.$$

$$+ \sum \frac{1}{v_{0n}} \left(\frac{2}{n\pi} \right)^2 \left(\frac{b_1}{b} \right) \left(\frac{b_2}{b} \right) \psi_{122} \psi'_{122}$$

$$\left. + \sum \sum \frac{1}{v_{mn}} \left(\frac{4}{mn\pi^2} \right)^2 \psi_{121} \psi'_{121} \psi_{122} \psi'_{122} \right]$$

$$\left. \cdot \frac{k}{k_z \sin k_z l} \right\} = (-1)^2 jU_2 Z_0 E_{12}, \qquad (4)_1$$

$$\overline{p}_{21} = (-1)^1 jU_1 Z_0 \left\{ \frac{1}{\sin kl} + \left(\frac{bh}{b_2 h_2} \right) \left(\frac{bh}{b_1 h_1} \right) \right.$$

$$\cdot \left[\sum \frac{1}{v_{m0}} \left(\frac{2}{m\pi} \right)^2 \left(\frac{h_2}{h} \right) \left(\frac{h_1}{h} \right) \psi_{211} \psi'_{211} \right.$$

$$+ \sum \frac{1}{v_{0n}} \left(\frac{2}{n\pi} \right)^2 \left(\frac{b_2}{b} \right) \left(\frac{b_1}{b} \right) \psi_{212} \psi'_{212}$$

$$\left. + \sum \sum \frac{1}{v_{mn}} \left(\frac{4}{mn\pi^2} \right)^2 \psi_{211} \psi'_{211} \psi_{212} \psi'_{212} \right]$$

$$\left. \cdot \frac{k}{k_z \sin k_z l} \right\} = (-1)^1 jU_1 Z_0 E_{21}, \qquad (4)_2$$

where

$$\psi_{121} = \sin \frac{m\pi b_1}{2b} \cos \frac{m\pi b_{c1}}{b},$$

$$\psi'_{121} = \sin \frac{m\pi b_2}{2b} \cos \frac{m\pi b_{c2}}{b},$$

$$\psi_{122} = \sin \frac{m\pi h_1}{2h} \cos \frac{m\pi h_{c1}}{h}$$

$$\psi'_{122} = \sin \frac{m\pi h_2}{2h} \cos \frac{m\pi h_{c2}}{h}$$

$$\psi_{221} = \sin \frac{m\pi b_2}{2b} \cos \frac{m\pi b_{c2}}{b}, \qquad (4)_3$$

$$\psi'_{221} = \sin \frac{m\pi b_1}{2b} \cos \frac{m\pi b_{c1}}{b},$$

$$\psi_{222} = \sin \frac{m\pi h_2}{2h} \cos \frac{m\pi h_{c2}}{h}$$

$$\psi'_{222} = \sin \frac{m\pi h_1}{2h} \cos \frac{m\pi h_{c1}}{h}.$$

By using the superposition method, the overall potential energy at the chamber inlet is

$$\overline{P}_1 = \overline{p}_{11} + \overline{p}_{12} = -jZ_0 \left(U_1 E_{11} - U_2 E_{12} \right). \qquad (5)$$

Similarly, the overall potential energy at the chamber outlet is

$$\overline{P}_2 = \overline{p}_{21} + \overline{p}_{22} = -jZ_0 \left(U_1 E_{21} - U_2 E_{22} \right). \qquad (6)$$

The acoustical transfer matrix between nodes 1 and 2 is

$$\begin{bmatrix} P_1 \\ U_1 \end{bmatrix} = \begin{bmatrix} T_{11} & T_{12} \\ T_{21} & T_{22} \end{bmatrix} \begin{bmatrix} P_2 \\ U_2 \end{bmatrix}. \qquad (7)$$

Developing Eq. (7) yields

$$P_1 = T_{11} P_2 + T_{12} U_2, \qquad (8)_1$$

$$U_1 = T_{21} P_2 + T_{22} U_2, \qquad (8)_2$$

$$\begin{aligned} T_{11} &= \left. (\overline{P}_1/\overline{P}_2) \right|_{U_2=0} = E_{11}/E_{12}, \\ T_{12} &= \left. (\overline{P}_1/U_2) \right|_{\overline{P}_2=0} = jZ_0 (E_{12} - E_{11} E_{22}/E_{12}). \\ T_{21} &= \left. (U_1/\overline{P}_2) \right|_{U_2=0} = j(Z_0 E_{12})^{-1}, \\ T_{22} &= \left. (U_1/U_2) \right|_{\overline{P}_2=0} = E_{22}/E_{12}, \end{aligned} \qquad (8)_3$$

where Pi and Ui are the acoustical potential energy and the volume velocity at the i-th node.

Consequently, the sound transmission loss (STL) of the muffler is

$$STL = 20 \log \left[\frac{\left| T_{11} + \dfrac{T_{12}}{Z_2} + T_{21} Z_1 + T_{22}(S_2/S_1) \right|}{2} \right], \qquad (9)_1$$

$$\begin{aligned} Z_1 &= \rho_0 c/S_1, & Z_2 &= \rho_0 c/S_2, \\ S_1 &= b_1 h_1, & S_2 &= b_2 h_2, \end{aligned} \qquad (9)_2$$

where Z_1 is the acoustic impedance of the inlet in z-axis, Z_2 is the acoustic impedance of the outlet in z-axis, S_1 is the section area of the inlet, and S_2 is the section area of the outlet.

2.2. Sound transmission loss of expansion chamber mufflers

Based on Subsec. 2.1, the acoustic performances of expansion chamber mufflers KA, KB, and KC will be established as follows:
For the mufflers KA, KB, and KC, the system's four-pole matrix and STL are

$$\begin{bmatrix} P_1 \\ U_1 \end{bmatrix}_{KA} = \begin{bmatrix} T_{11} & T_{12} \\ T_{21} & T_{22} \end{bmatrix}_{KA} \begin{bmatrix} P_2 \\ U_2 \end{bmatrix}_{KA}, \qquad (10)_1$$

$$\begin{bmatrix} P_1 \\ U_1 \end{bmatrix}_{KB} = \begin{bmatrix} T_{11} & T_{12} \\ T_{21} & T_{22} \end{bmatrix}_{KB} \begin{bmatrix} P_2 \\ U_2 \end{bmatrix}_{KB}, \qquad (10)_2$$

$$\begin{bmatrix} P_1 \\ U_1 \end{bmatrix}_{KC} = \prod_{m=1}^{3} [T_m(f)]_{KC} \begin{bmatrix} P_4 \\ U_4 \end{bmatrix}_{KC}, \qquad (10)_3$$

$STL_{KA}(f, \overline{X}_{KA})$

$$= 20 \log \left[\frac{\left| T_{11} + \dfrac{T_{12}}{Z_2} + T_{21}Z_1 + T_{22}(S_2/S_1) \right|}{2} \right]_{KA}, \quad (10)_4$$

$STL_{KB}(f, \overline{X}_{KA})$

$$= 20 \log \left[\frac{\left| T_{11} + \dfrac{T_{12}}{Z_2} + T_{21}Z_1 + T_{22}(S_2/S_1) \right|}{2} \right]_{KB}, \quad (10)_5$$

$STL_{KC}(f, \overline{X}_{KC})$

$$= 20 \log \left[\frac{\left| T_{11} + \dfrac{T_{12}}{Z_2} + T_{21}Z_1 + T_{22}(S_4/S_1) \right|}{2} \right]_{KC}, \quad (10)_6$$

$$
\begin{aligned}
\overline{X}_{KA} &= (A_o, A_1, L_o), \\
\overline{X}_{KB} &= (B_o, H_o, L_o), \\
\overline{X}_{KC} &= (L_1, L_2, L_3, B_o), \\
A_o &= B_o \cdot H_o, \\
A_1 &= B_1 \cdot H_1, \\
B_1 &= B_2 = H_1 = H_2,
\end{aligned}
\qquad (10)_7
$$

where $T_m(f)$ is the m-th four-pole transfer matrix between nodes m and $m+1$, Si is the section area of the i-th node, and Li is the i-th horizontal span of the muffler KC.

2.3. Objective function

By using the formulas of Eq. (10), the objective functions used in the GA optimization with respect to each type of muffler are established. For the mufflers KA, KB, and KC, the objective function in maximizing the STL at one tone (f_1) is

$$
\begin{aligned}
OBJ_{KA} &= STL_{KA}(f_1, \overline{X}_{KA}), \\
OBJ_{KB} &= STL_{KB}(f_1, \overline{X}_{KB}), \\
OBJ_{KC} &= STL_{KC}(f_1, \overline{X}_{KC}).
\end{aligned}
\qquad (11)
$$

3. Model check

Before performing the *GA* optimal simulation on expansion chamber mufflers, an accuracy check of the mathematical models on mufflers (A: a concentric straight expansion chamber muffler; B: a bias straight expansion chamber muffler; C: a reverse expansion chamber muffler) shown in Fig. 4 is performed using the analytic solution from IH (1992). As depicted in Figs. 5, 6 and 7, the theoretical prediction
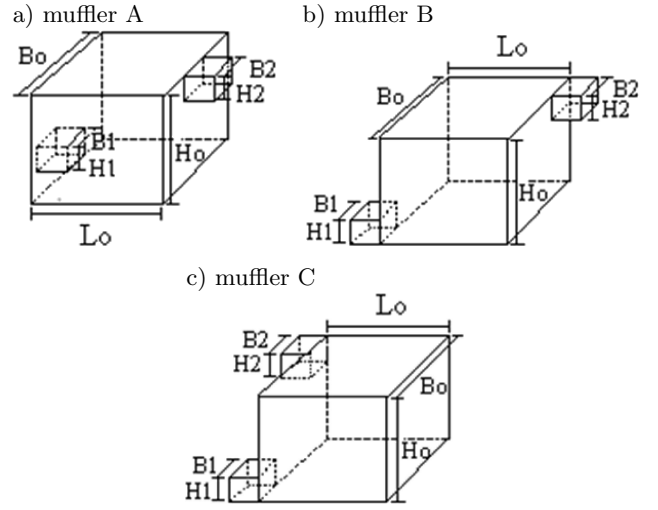
a) muffler A   b) muffler B

c) muffler C

Fig. 4. Mechanisms for three kinds of expansion chamber mufflers (muffler A: a concentric straight expansion chamber muffler; muffler B: a bias straight expansion chamber muffler; muffler C: a reverse expansion chamber muffler).
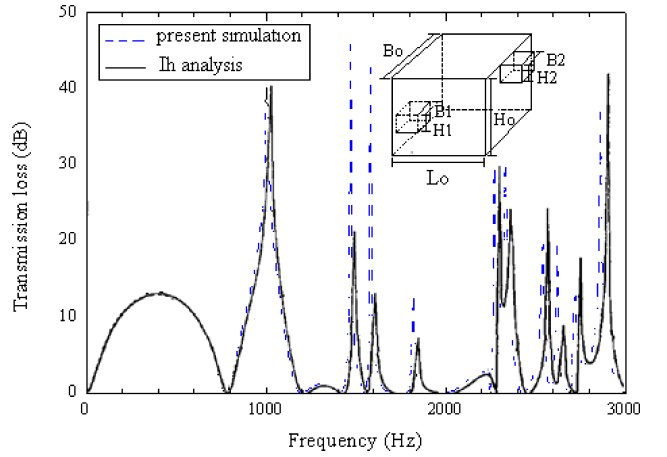

Fig. 5. Comparison of the simulated results of a concentric straight expansion chamber muffler with Ih's analytic solution (muffler A: Bo=Ho=0.15 m, B1=B2=H1=H2=0.05 m, Lo=0.025 m) (IH, 1992).
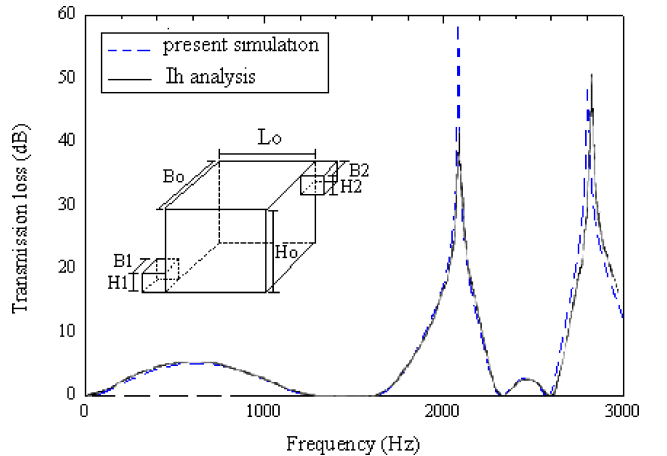

Fig. 6. Comparison of the simulated results of a bias straight expansion chamber muffler with Ih's analytic solution (muffler B: Bo=Ho=0.15 m, B1=B2=H1=H2=0.05 m, Lo=0.025 m) (IH, 1992).
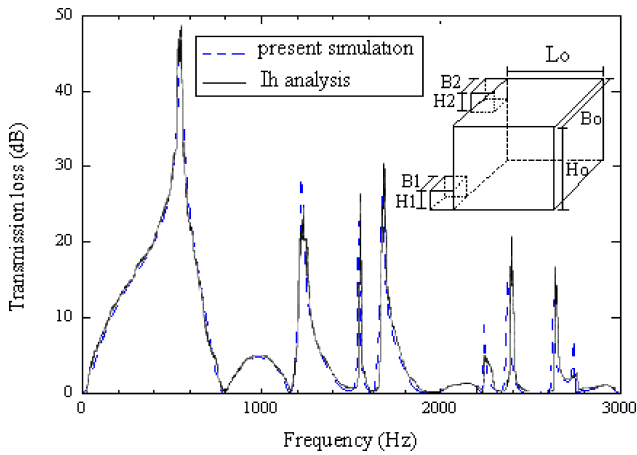
Fig. 7. Comparison of the simulated results of a reverse expansion chamber muffler with Ih's analytic solution (muffler C: Bo=Ho=0.15 m, B1=B2=H1=H2=0.05 m, Lo=0.025 m) (Iн, 1992).

from Eq. (10) and Ih's analytic data are in agreement. Therefore, the proposed fundamental mathematical models for the one-chamber mufflers with inlets and outlets on the same side and on opposite sides are acceptable. Consequently, the models linked with the numerical method are applied to the shape optimization of mufflers KA-KC shown in Fig. 3 in the following section.

4. Case studies

There are three kinds of primary pure tones (500 Hz, 1000 Hz, and 2000 Hz) occurring in three venting pieces of equipment. In order to reduce the individual pure tone noise, three kinds of mufflers (KA-KC) with simple mechanisms shown in Fig. 3 are

Table 1. Constrained conditions in the mufflers.

muffler KA		
Design Parameters	Min. [m]	Max. [m]
L0	0.20	0.40
A0	0.10*0.10	0.30*0.30
A1	0.05*0.05	0.10*0.10
muffler KB		
Design Parameters	Min. [m]	Max. [m]
L0	0.20	0.40
B0	0.10	0.30
H0	0.10	0.30
muffler KC		
Design Parameters	Min. [m]	Max. [m]
L1	0.05	0.15
L2	0.05	0.15
L3	0.05	0.15
B0	0.10	0.30

adopted where KA is a concentric straight expansion chamber muffler, KB is a reverse straight expansion chamber muffler, and KC is a straight expansion chamber muffler hybridized with two baffles. The heights (HH1 and HH2) of the baffles are fixed at 0.1 m.

Obtaining the best acoustic performance by adjusting the design parameters, numerical assessments linked to a GA optimizer are applied. There are three kinds of targeted tones (500 Hz, 1000 Hz, and 2000 Hz) used in the optimization. The corresponding OBJ functions and ranges of the design parameters are summarized in Eq. (11) and Table 1.

5. Genetic algorithm

A genetic algorithm (GA) used to search for the global optimum by imitating a genetic evolutionary process was first formalized by Holland (1975) and later extended to functional optimization by Jong (1975). It has been widely used in various fields (Chiu, Chang, 2008; Chiu, 2010a; 2010b). The main advantages of the GA include the following: (1) solutions coded as bit strings (chromosomes) in which large problems can be easily handled by using long strings; (2) genetic operations such as crossover, mutation, and elitism, which are very easy to apply; (3) a mating pool of chromosomes.

In this paper, for the optimization of the objective function (OBJ), the design parameters of $(X_1, X_2, \ldots, X_k)$ were determined. When the bit (the bit length of the chromosome) and the pop (the population number) were chosen, the interval of the k-th design parameter (X_k) with $[Lb, Ub]_k$ was then mapped to the band of the binary value. The initial population was randomly built up. The parameter set was encoded to form a string that represented the chromosome. By evaluating the objective function (OBJ), the whole set of chromosomes $[B2D_1, B2D_2, \ldots, B2D_k]$ that changed from a binary to a decimal form was then assigned a fitness by decoding the transformation system. As it can be seen in Fig. 8, one pair of offspring was generated from the selected parent using a uniform crossover with a probability of pc during the GA optimization. Hereditarily, mutation occurred with a probability of pm in which the new and unexpected point was brought into the GA's optimizer search domain. To prevent the best gene from disappearing and to improve the accuracy of optimization during reproduction, the elitism scheme for keeping the best gene in the parent generation using a tournament strategy was adopted. As indicated in Fig. 9, the process was terminated when the number of generations reached a pre-selected value of $iter_{\max}$. The GA optimization has been programmed in Fortran and run on an IBM PC.
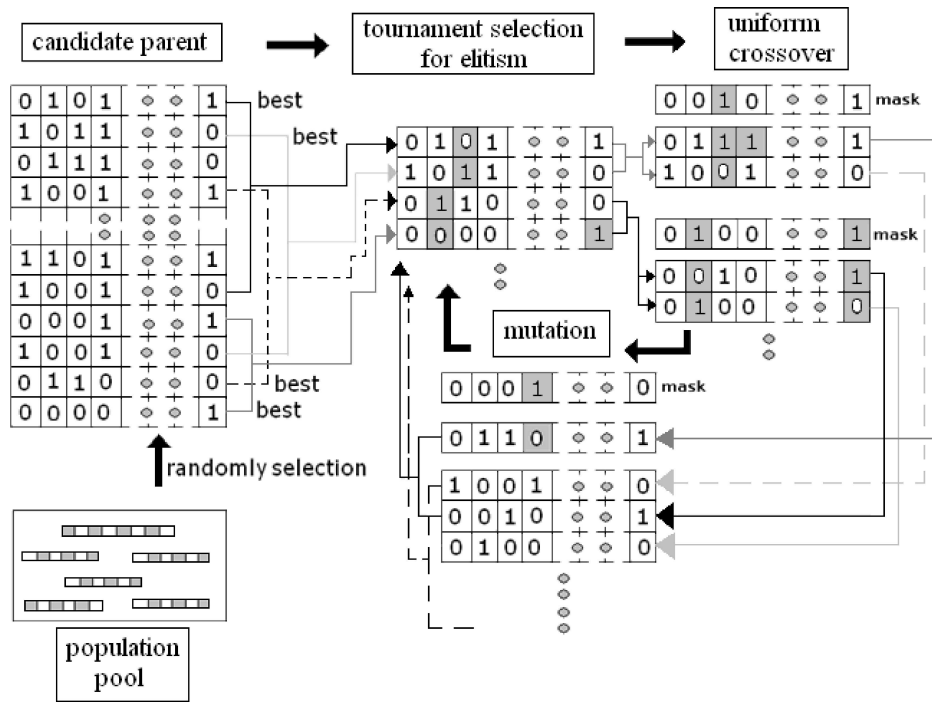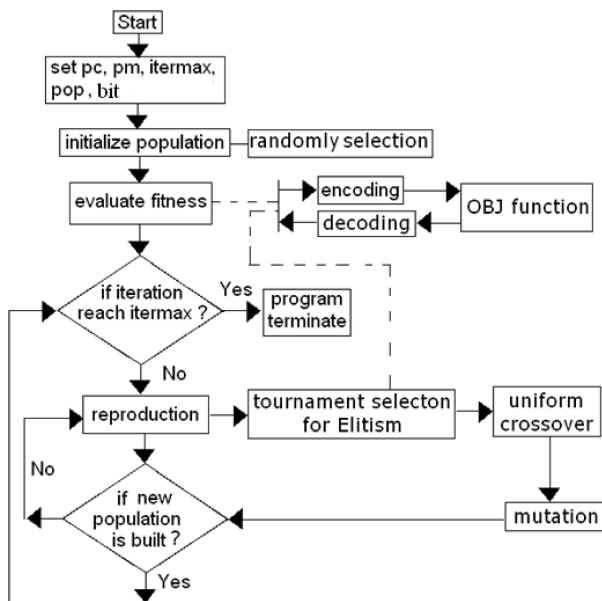
Fig. 8. Operations of the *GA* method.

Fig. 9. Flow chart of the *GA*.

6. Results and discussion

6.1. Results

The accuracy of the *GA* optimization depends on five types of *GA* parameters that include *pop* (population number), *bit* (chromosome length), *pc* (crossover rate), *pm* (mutation factor), and *iter*$_{max}$ (maximum iteration). To achieve a good optimization, the following parameters are varied step by step. The related GA control parameters used in the optimization are shown in Table 2.

Table 2. Selected GA parameters during shape optimization.

GA parameters	Value (or condition)
bit	20
pop	50
elitism	(tournament)
crossover	(uniform crossover)
pc	0.5
pm	0.5
iter$_{max}$	1000

Considering Eqs. (10) and (11) and using the *GA* parameters in the optimization process, the maximization of the $STL_{KA} \sim STL_{KC}$ with respect to mufflers KA~ KC at three targeted tones (500 Hz, 100 Hz, and 200 Hz) was performed and shown in Tables 3–5. As illustrated in Table 3, the *STL* of the muffler KA at 500 Hz, 1000 Hz, and 2000 Hz has been improved from 11 dB, 18 dB, 4 dB to 25 dB, 25 dB, and 52 dB. Similarly, as illustrated in Table 4, the *STL* of the muffler KB at 500 Hz, 1000 Hz, and 2000 Hz has been improved from 15 dB, 6 dB, 5 dB to 72 dB, 49 dB, and 42 dB. Likewise, Table 5 indicates that the *STL* of the muffler KC at 500 Hz, 1000 Hz, and 2000 Hz has been improved from 10 dB, 20 dB, 44 dB to 28 dB, 95 dB, and 115 dB.

Table 3. Comparison of *STL* and design parameters of the muffler KA before and after the optimization.

Target tone		Design Parameters			OBJ
		L0	A0	A1	STL_{KA} [dB]
500 Hz	original	0.30	0.20*0.20	0.05*0.05	11
	optimization	0.2054	0.2991*0.2991	0.0509*0.0509	25
1000 Hz	original	0.30	0.20*0.20	0.05*0.05	18
	optimization	0.3959	0.2992*0.2992	0.0507*0.0507	25
2000 Hz	original	0.30	0.20*0.20	0.05*0.05	4
	optimization	0.2447	0.2709.0.2709	0.0550*0.0550	52

Table 4. Comparison of STL and design parameters of the muffler KB before and after the optimization.

Target tone		Design Parameters			OBJ
		L0	B0	H0	STL_{KB} [dB]
500 Hz	original	0.30	0.20	0.20	15
	optimization	0.2836	0.2888	0.2566	72
1000 Hz	original	0.30	0.20	0.20	6
	optimization	0.2974	0.1713	0.1829	49
2000 Hz	original	0.30	0.20	0.20	5
	optimization	0.2637	0.1321	0.2227	42

Table 5. Comparison of *STL* and design parameters of the muffler KC before and after the optimization.

Target tone		Design Parameters				OBJ
		L1	L2	L3	B0	STL_{KC} [dB]
500 Hz	original	0.10	0.10	0.10	0.20	10
	optimization	0.1491	0.1470	0.0879	0.2993	28
1000 Hz	original	0.10	0.10	0.10	0.20	20
	optimization	0.1475	0.1376	0.1415	0.1959	95
2000 Hz	original	0.10	0.10	0.10	0.20	44
	optimization	0.1473	0.0521	0.1300	0.1286	115

Using this optimal design in a theoretical calculation, the optimal *STL* curves with respect to the muffler KA at targeted tones (500 Hz, 1000 Hz, and 2000 Hz) are plotted in Figs. 10–12. Equally, the optimal *STL* curves with respect to the muffler KB at targeted tones (500 Hz, 1000 Hz, and 2000 Hz) are plotted in Figs. 13–15. Consequently, the optimal *STL* curves with respect to the muffler KC at targeted tones (500 Hz, 1000 Hz, and 2000 Hz) are plotted in Figs. 16–18.

6.2. Discussion

As indicated in Figs. 10–18, the STLs of the expansion chamber mufflers have been precisely maximized at the targeted tones. As illustrated in Table 3, the *STL* of the muffler KA at 500 Hz, 1000 Hz, and
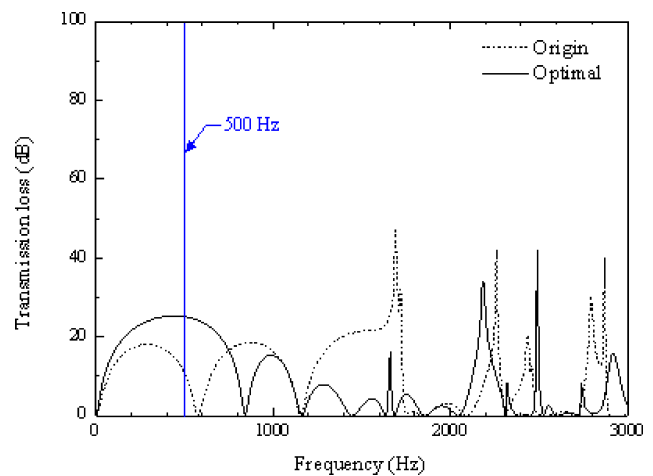

Fig. 10. Comparison of the *STL* of the muffler KA before and after optimization is performed (target tone: 500 Hz).
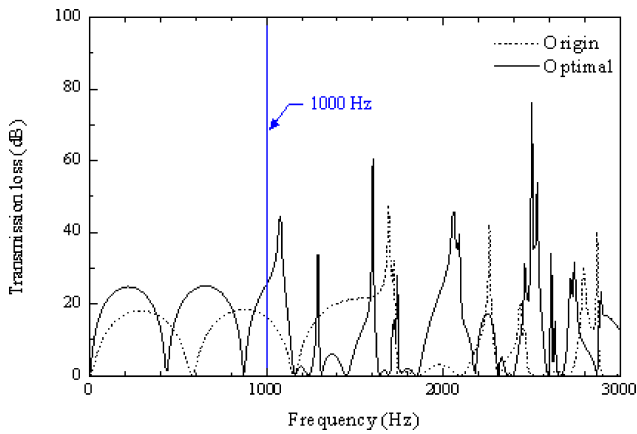
Fig. 11. Comparison of the *STL* of the muffler KA before and after optimization is performed (target tone: 1000 Hz).
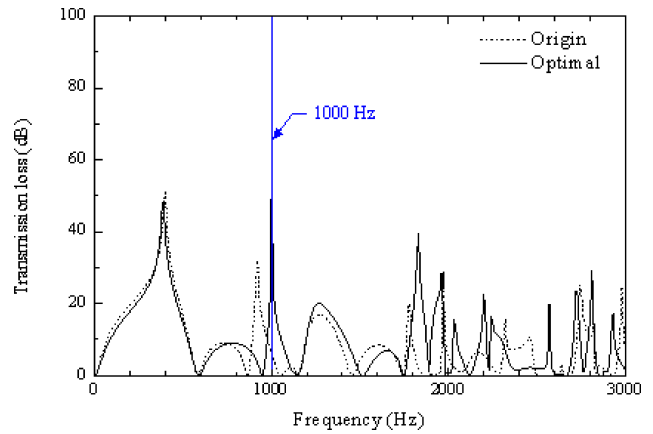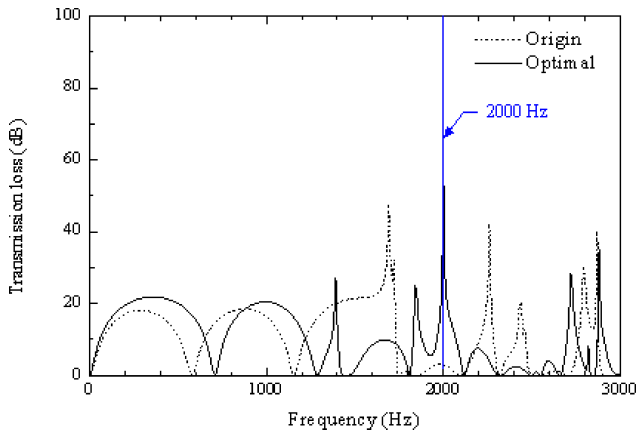

Fig. 12. Comparison of the *STL* of the muffler KA before and after optimization is performed (target tone: 2000 Hz).
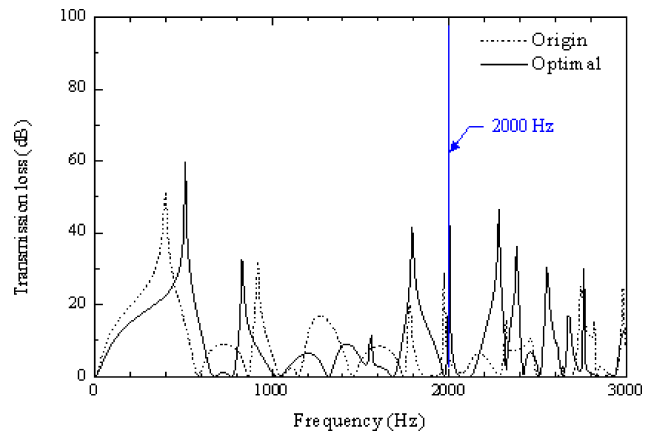

Fig. 13. Comparison of the *STL* of the muffler KB before and after optimization is performed (target tone: 500 Hz).

Fig. 14. Comparison of the *STL* of the muffler KB before and after optimization is performed (target tone: 1000 Hz).

Fig. 15. Comparison of the *STL* of the muffler KB before and after optimization is performed (target tone: 2000 Hz).
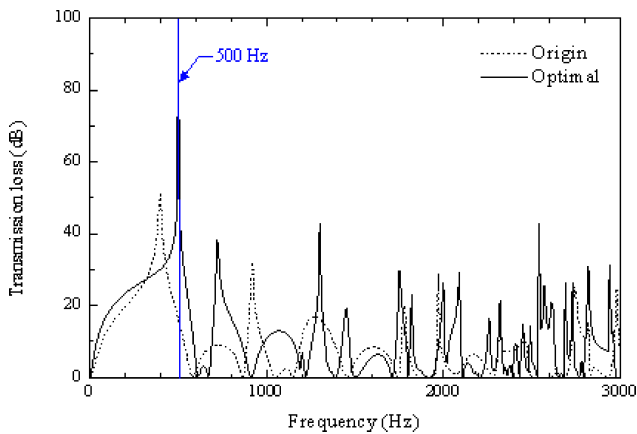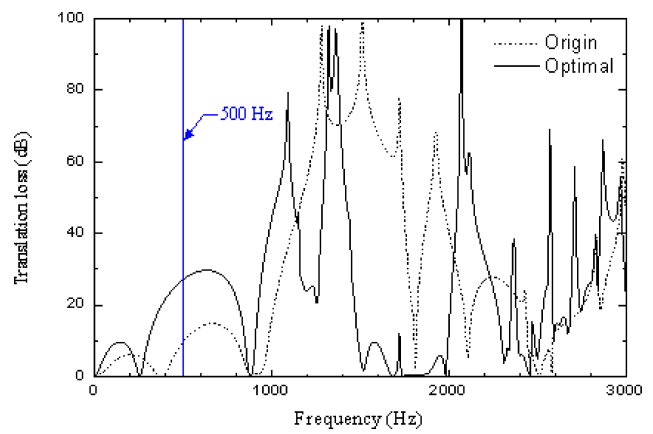

Fig. 16. Comparison of the *STL* of the muffler KC before and after optimization is performed (target tone: 500 Hz).

2000 Hz has been increased by 14 dB, 7 dB, and 48 dB after the shape optimization process. Similarly, Table 4 indicates that the *STL* of the muffler KB at 500 Hz, 1000 Hz, and 2000 Hz has been increased by 57 dB, 43 dB, and 37 dB when performing the optimization process. Likewise, Table 5 indicates that the *STL* of the muffler KC at 500 Hz, 1000 Hz, and 2000 Hz has

been improved by 18 dB, 75 dB, and 71 dB with the GA optimization.

As indicated in Figs. 5 and 6, for a straight expansion chamber muffler (mufflers A and B) with a fixed outline size, the profile of the *STL* will be shifted and the influence of the overall acoustic performance will be limited when adjusting the allocation of the inlet
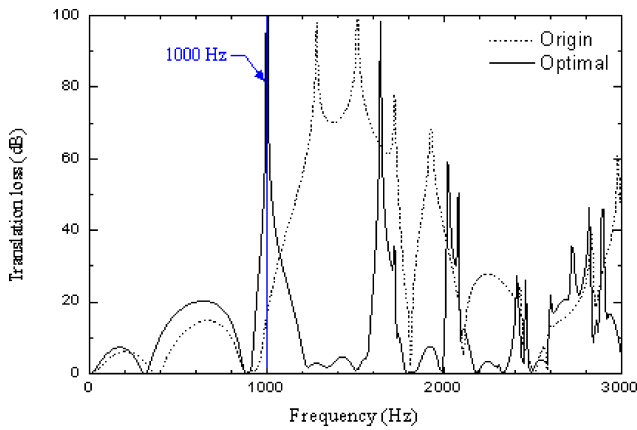
Fig. 17. Comparison of the *STL* of the muffler KC before and after optimization is performed (target tone: 1000 Hz).
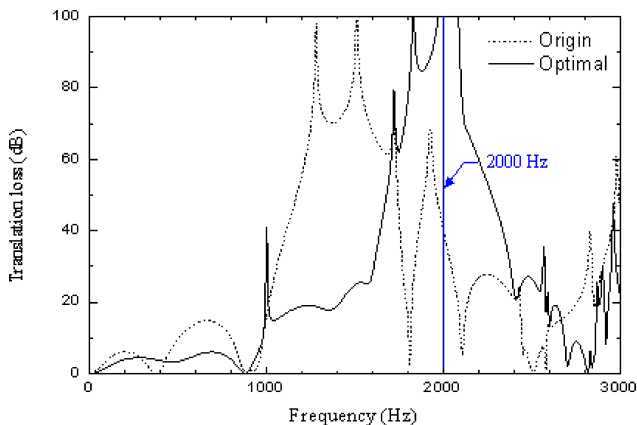

Fig. 18. Comparison of the *STL* of the muffler KC before and after optimization is performed (target tone: 2000 Hz).

and outlet. As indicated in Fig. 7, the overall acoustic performance will be improved when both the inlet and outlet are located on the same side (muffler C: a reverse expansion chamber muffler).

To realize the acoustical influence with respect to different types of expansion chamber mufflers, three kinds of mufflers (KA-KC) are adopted and optimized at three targeted tones (500 Hz, 1000 Hz, and 2000 Hz) by adjusting the outline dimensions of the mufflers via the GA optimizer. Figures 10–15 reveal that the overall *STL* of the muffler KB (a reverse expansion chamber muffler with one chamber) is larger than that of the muffler KA (a straight expansion chamber muffler with one chamber). Also, Figs. 10–12 and Figs. 16–18 indicate that the overall *STL* of the muffler KC (a straight expansion chamber muffler partitioned to three chambers with two baffles) is larger than that of the muffler KA (a straight expansion chamber muffler with one chamber).

Consequently, the acoustic performance of a straight expansion chamber muffler partitioned to three chambers with two baffles is superior to the other two mufflers (a straight and a reverse expansion chamber ones).

7. Conclusion

It has been shown that the optimization of expansion chamber muffler shapes can be easily and efficiently carried out by using a four-pole transfer matrix as well as a *GA* optimizer. As indicated in Figs. 10–18, the predicted maximum value of the *STL* is precisely located at the desired frequency. Hence, the tuning ability established by adjusting the design parameters of mufflers KA-KC is reliable. In addition, as indicated in Figs. 5 and 6, the influence of the overall acoustic performance for a one-chamber expansion chamber muffler with a fixed volume and fixed inlet/outlet sections will be small when adjusting the allocation of the inlet and outlet. Also, as indicated in Fig. 7, the overall acoustic performance of a one-chamber expansion chamber muffler with a fixed volume and fixed inlet/outlet sections will be improved when both the inlet and outlet are located on the same side.

Furthermore, as indicated in Figs. 10–18, optimal results reveal that the muffler KC is superior to the other mufflers. It can be seen that the acoustic performance of a reverse expansion chamber muffler is better than that of a straight expansion chamber muffler. In addition, more chambers in the muffler will result in a better acoustic performance.

Consequently, considering the higher order mode of the sound wave, the approach used for the optimal noise elimination of pure tones for various kinds of expansion chamber mufflers proposed in this study is quite important and can be efficiently achieved

References

1. Abom M. (1990), *Derivation of four-pole parameters including higher order mode effects for expansion chamber mufflers with extended inlet and outlet*, Journal of Sound and Vibration, **137**, 403–418.

2. Chang Y.C., Yeh L.J., Chiu M.C. (2004), *GA optimization on constrained venting system with single-chamber mufflers*, Journal of the Acoustical Society of R.O.C., **10**, 1–13.

3. Chang Y.C., Yeh L.J., Chiu M.C. (2004), *Optimization of absorbers and mufflers on constrained multi-noises system by using genetic algorithm*, The Far East Journal of Applied Mathematics, **14**, 3, 261–299.

4. Chiu M.C. (2010), *Shape optimization of multi-chamber mufflers with plug-inlet tube on a venting process by genetic algorithms*, Applied Acoustics, **71**, 495–505.

5. Chiu M.C. (2010), *Shape optimization of one-chamber mufflers with reverse-flow ducts using a genetic algorithm*, Journal of Marine Science and Technology, **18**, 1, 12–23.

6. Chiu M.C., Chang Y.C. (2008), *Numerical studies on venting system with multi-chamber perforated mufflers by GA optimization*, Applied Acoustics, **69**, 11, 1017–1037.

7. DAVIS D.D., STOKES J.M., MOORE D., STEVEN L. (1954), *Theoretical and experimental investigation of mufflers with comments on engine exhaust muffler design*, NACA Report 1192.

8. ELSAADANY S., ELNADY T., BOIJ S., ABOM M. (2011), *Optimization of exhaust systems to meet the acoustic regulations and the engine specifications*, ICSV18, Rio de Janeiro 10–14 July 2011.

9. HARTIG H.E., SWANSON C.E. (1938), *Transverse acoustic waves in rigid tubes*, Physical Review **54**, 618–626.

10. HOLLAND J. (1975), *Adaptation in natural and artificial system*, Ann Arbor, University of Michigan Press.

11. IGARASHI J., ARAI M. (1960), *Fundamentals of acoustical silencers, part 3: Attenuation characteristic studies by electric simulator*, Aeronaut Res. Inst. University of Tokyo, Report No. 351, 17–31.

12. IGARASHI J., TOYAMA M. (1958), *Fundamentals of acoustical silencers, part 1: Theory and experiment of acoustic low-pass filters*, Aeronaut Res. Inst. University of Tokyo, Report No. 339, 223–241.

13. IH J.G. (1992), *The reactive attenuation of rectangular plenum chambers*, Journal of Sound and Vibration, **157**, 93–122.

14. IH J.G., LEE B.H. (1985), *Analysis of higher-order mode effects in the circular expansion chamber with mean flow*, Journal of the Acoustical Society of America, **77**, 1377–1388.

15. IH J.G., LEE B.H. (1987), *Theoretical prediction of the transmission loss of circular reversing chamber mufflers*, Journal of Sound and Vibration, **112**, 261–272.

16. JAYARAMAN K., YAM K. (1981), *Decoupling approach to modeling perforated tube muffler components*, Journal of the Acoustical Society of America, **69**, 2, 390–396.

17. JONG D. (1975), *An analysis of the behavior of a class of genetic adaptive Systems*, Doctoral Dissertation, Department of Computer and Communication Sciences, Ann Arbor, University of Michigan, USA.

18. MILES J. (1944), *The reflection of sound due to a change in cross section of a circular tube*, Journal of the Acoustical Society of America, **16**, 14–19.

19. MIWA T., IGARASHI J. (1959), *Fundamentals of acoustical silencers, part 2: Determination of four terminal constants of acoustical element*, Aeronaut Res. Inst. University of Tokyo, Report No. 344, 67–85.

20. MUNJAL M.L. (1957), *Velocity ratio-cum-transfer matrix method for the evaluation of a muffler with mean flow*, Journal of the Acoustical Society of America, **39**, 105–119.

21. MUNJAL M.L. (1987), *A simple numerical method for three-dimensional analysis of simple expansion chamber mufflers of rectangular as well as circular cross-section with a stationary medium*, Journal of Sound and Vibration, **116**, 71–88.

22. SEYBERT A.F., CHENG C.Y.R. (1987), *Application of the boundary element method to acoustic cavity response and muffler analysis*, Transactions of the American Society of Mechanical Engineers, Journal of Vibration, Stress, and Reliability in Design **109**, 15–21.

23. STRUT J.W. (RAYLEIGH L.) (1945), *The theory of sound*, Dover New York.

24. SULLIVAN J.W., CROCKER M.J. (1978), *Analysis of concentric-tube resonators having unpartitioned of cavities*, Journal of the Acoustical Society of America, **64**, 1, 207–215.

25. SULLIVAN J.W. (1979), *A method for modeling perforated tube muffler components. I. theory*, Journal of the Acoustical Society of America, **66**, 3, 772–778.

26. YOUNG C.I., CROCKER M.J. (1975), *Prediction of transmission loss in mufflers by the finite-element method*, Journal of the Acoustical Society of America, **57**, 144–148.